IEEE Access
Multidisciplinary | Rapid Review | Open Access Journal

Received December 4, 2019, accepted January 21, 2020, date of current version March 23, 2020.

Digital Object Identifier 10.1109/ACCESS.2020.2974938

Operation Cost Optimization on an Ultralow Emission System Based on Improved Collaborative Optimization

SONG ZHENG[1], KAFEI TANG[1], SHUAI CHEN[2], AND XIAOQING ZHENG[2]

[1]School of Automation, Hangzhou Dianzi University, Hangzhou 310018, China
[2]Engineering Research Center of Measuring Instrument and Integration Technology for Automation System, Ministry of Education, Hangzhou Dianzi University, Hangzhou 310018, China

Corresponding author: Song Zheng (zhs@hdu.edu.cn)

This work was supported in part by the National Natural Science Foundation of China under Grant U1609212 and Grant 61304211, in part by the Belt and Road International S&T Cooperation Project of Zhejiang Province under Grant 2019C4021, and in part by the Public Technology Research Project of Zhejiang Province under Grant LGG20F030002.

ABSTRACT Due to the lack of an effective overall coordinated treatment method, it is difficult to achieve low cost and efficient removal of pollutants from coal-fired flue gas. This paper establishes a collaborative optimization model for ultralow emission systems, including a system level model of operation cost and three discipline level models for denitration, desulfurization, and dust removal. An improved collaborative optimization method with a dynamic penalty function is proposed to optimize an ultralow emission system. Simulation results show that the improved method achieves better global optimization and effectively reduces the operation cost of the system under ultralow emission constraints.

INDEX TERMS Coal-fired flue gas pollutant, collaborative removal, dynamic penalty function, collaborative optimization, operation cost.

I. INTRODUCTION

Due to the continuous enhancement of environmental protection requirements, ultralow emission systems for coal-fired power plants (ULE system) are constantly being updated and improved. At present, there are many studies and optimizations of various equipment used in coal- burning flue gas emission systems in the relevant literature. For denitrification devices, Peng et al. established the exponential ARMAX model of the denitrification process and proposed a corresponding generalized predictive control strategy [1]. Subsequently, Peng et al. established an ARX nonlinear model of the denitrification process based on a radial basis function and proposed a corresponding model predictive control strategy [2]. Regarding desulfurization devices, Perales et al. controlled the outlet concentration of SO_2 and absorber slurry via the dynamic matrix control method [3]. Li constructed an improved neural network PID control algorithm with a prediction model based on the LM algorithm to control the slurry value [4]. With respect to dedusting devices, Xu adopted a k-means clustering algorithm based on the RBF neural network, which determined the electric dust collector export concentration and a mathematical model for secondary voltage; a genetic algorithm was used to study the optimization strategy for saving energy [5]. Grass implemented fuzzy control of operating voltage according to the change of load size based on expert experience rules and achieves better economic operation, energy savings and consumption reduction [6]. Using the k-means clustering algorithm of the RBF neural network, Li et al. obtained a mathematical model of the outlet concentration and secondary voltage of the electrostatic precipitator [7]. However, there are few studies on the synergistic function and operation cost optimization of ULE system.

The problem of collaborative optimization of the dewatering process for ULE system, which involves multiple professional models such as denitration, desulfurization, dedusting, etc., belongs to the field of multimodel complex system optimization; there are also collaborative dedusting effects between devices. At present, the solving strategies for complex multimodel systems can be divided into two categories: centralized and decentralized decision strategies [8]. For centralized decision strategies, multiple models are combined into a single model to solve the problem; this is effective

The associate editor coordinating the review of this manuscript and approving it for publication was Kai Li.

only when the coupling between models is relatively simple, and different models in the system can be integrated. When the degree of coupling is increased or when different models based on different methods cannot be integrated, a centralized decision system is difficult to solve, update and maintain. A decentralized decision system is more suitable for this situation. Decentralized decision decouples the coupled models and solves each of the models separately. Kroo et al. proposed a new approach, collaborative optimization (CO), which is considered a kind of advanced decentralized solving strategy. This approach decomposes the problem into two levels of optimized structure, and it has high degree of autonomy and good adaptability, suitable for optimization problems of multimodel complex systems such as reducers. CO has been successfully applied to many practical engineering design problems. For example, it has been used in the conceptual design of launch vehicles [9], high-speed civil transportation [10], space aircraft [11], aircraft wings [12], undersea vehicles [13], and excavators [14]. Although there are many advantages to using CO, the features of the framework cause some difficulties [15]. For example, CO may have difficulty finding a viable solution under system level constraints. Therefore, the following techniques are introduced: (1) using an inequality constraint instead of an equality constraint to study the determination of a reasonable relaxation factor [16]; (2) using a penalty function method to obtain an approximate solution [17]; (3) using the response surface method to estimate the equation constraint and solve the approximate model [18]. However, most previous improvements to the CO algorithm focused on system level optimization and ignored discipline level optimization. Therefore, an improved collaborative optimization method based on a dynamic penalty function is proposed in this paper.

The organization of this paper is as follows: In section 2, the operation cost model for the ULE system is introduced. Section 3 presents the improved collaborative optimization with a dynamic penalty function and describes the model of the ULE system for a collaborative optimization strategy. Simulation tests and results are discussed in section 4, and conclusions are drawn in section 5.

II. OPERATION COST MODEL FOR COLLABORATIVE REMOVAL IN A ULE SYSTEM

The main components of a ULE system are a selective catalytic reduction system (SCR), an electrostatic precipitator (ESP), a wet flue gas desulfurization system (WFGD) and a wet electrostatic precipitator (WESP). The flow chart of the collaborative removal of pollutants from ULE system is shown in Fig. 1.

In the figure, the SCR uses the selective reduction of nitrogen oxide *NOx* by ammonia gas with a catalyst to reduce *NOx* to N_2, and thereby achieve the efficient removal of *NOx*. The ESP mainly utilizes a high-voltage electrostatic field. When the dust-containing gas passes through the high-voltage electrostatic field, it is electrically separated. The particulate matter generates a negatively charged band when it collides and combines with the negative ions, and then due to the force of the electric field, it discharges and deposits the dust to the anode surface, where it is finally collected by mechanical means. The WFGD washes the flue gas in the absorption tower, primarily via a large flow of circulating limestone/gypsum slurry, the sulfur oxides SO_x in the absorption flue gas react with limestone to form calcium sulfite, etc., and the gas is oxidized into byproducts such as calcium sulfate in the slurry tank. When SO_2 is effectively removed, *NOx* and *PM* pollutants can be collaboratively removed by slurry washing [19], [20].

The WESP and ESP operate in a similar way: *PM* is charged by high-voltage corona discharge, and the charged *PM* is drawn to the dust–collecting plate by the electric field. Then, with continuous or regular flushing, the *PM* will be cleared as the flushing fluid flows. Additionally, WESP can synergistically remove SO_2 at the same time [21]. The collaborative elimination process of *NOx*, SO_2 and *PM* can be represented by the following models:

NOx is removed [19]:

$$C_{NOx_{SCR_{out}}} = C_{NOx_{in}} \times S\left(x_{SCR_1}, \ldots, x_{SCR_i}\right) \quad (2\text{-}1)$$

where C_{NOx_in} represents the concentration of *NOx* produced by burning coal. $C_{NOx\_SCR\_out}$ is the export concentration of *NOx* after SCR, and $x_{SCR\_1}, \ldots, x_{SCR\_i}$ represent denitrification-related variables in SCR.

NOx is collaboratively removed by WFGD after removal by SCR:

$$C_{NOx_{out}} = C_{NOx_{SCR_{out}}} \times S\left(x_{WFGD_1}, \ldots, x_{WFGD_i}\right) \quad (2\text{-}2)$$

where C_{NOx_out} represents the exit concentration of *NOx* after coordinated elimination and $x_{WFGD\_1}, \ldots, x_{WFGD\_i}$ represent desulfurization-related variables in WFGD.

SO_2 is removed [20]:

$$C_{SO_{2WFGD_{out}}} = C_{SO_{2in}} \times S\left(x_{WFGD_1}, \ldots, x_{WFGD_i}\right) \quad (2\text{-}3)$$

where $C_{SO_2\_in}$ is the concentration of SO_2 produced by burning coal and $C_{SO_2\_WFGD\_out}$ is the export concentration of SO_2 after WFGD.

SO_2 is collaboratively removed by WESP after removal by WFGD:

$$C_{SO_{2out}} = C_{SO_{2WFGD_{out}}} \times S\left(x_{WESP_1}, \ldots, x_{WESP_i}\right) \quad (2\text{-}4)$$

where $C_{SO_2\_out}$ represents the exit concentration of SO_2 after coordinated elimination and $x_{WESP\_1}, \ldots, x_{WESP\_i}$ represent dust-related variables in WESP.

PM is removed [21]:

$$C_{PM_{in}} C_{NOx_{SCR_{out}}} = C_{PM_{ESP_{out}}} \times S\left(x_{ESP_1}, \ldots, x_{ESP_i}\right) \quad (2\text{-}5)$$

where C_{PM_in} is the concentration of *PM* produced by burning coal.

$C_{PM\_ESP\_out}$ is the exit concentration of *PM* after ESP and $x_{ESP\_1}, \ldots, x_{ESP\_i}$ represent dust-related variables in ESP.

Similarly, PM is collaboratively removed by WFGD after removal by ESP:

$$C_{PM\_WFGD\_out} = C_{PM\_ESP\_out} \times S(x_{WFGD\_1}, \ldots, x_{WFGD\_i}) \quad (2\text{-}6)$$

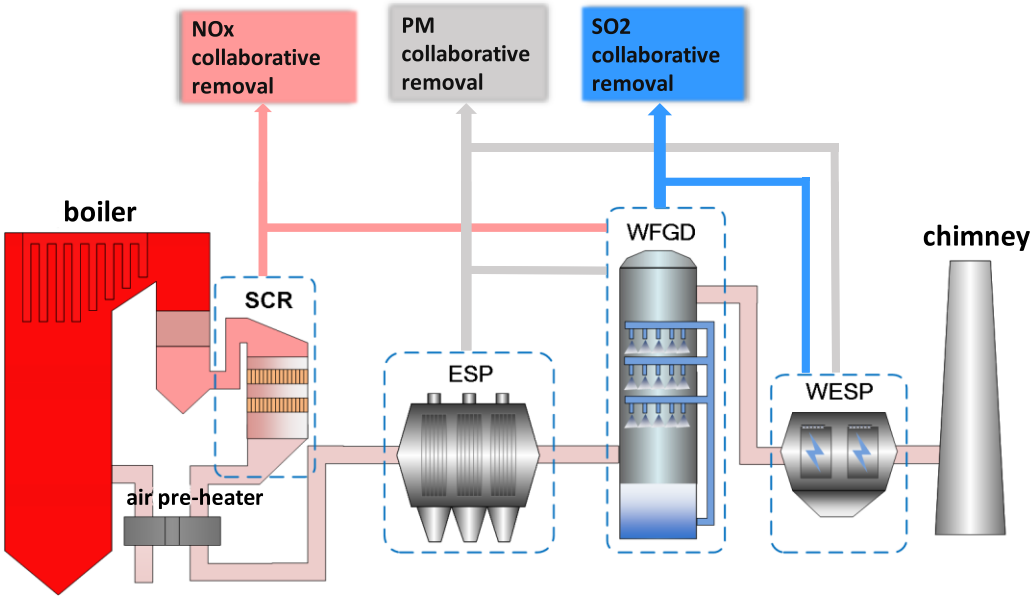

FIGURE 1. Flow chart of collaborative removal of pollutants from ULE system in coal-fired power plants.

where $C_{PM\_WFGD\_out}$ represents the export concentration of PM after WFGD combined with dust removal.

Then, PM is collaboratively removed by WESP:

$$C_{PM_{out}} = C_{PM_{WFGD_{out}}} \times S\left(x_{WESP_1}, \ldots, x_{WESP_i}\right) \quad (2\text{-}7)$$

where C_{PM_out} represents the exit concentration of PM after coordinated elimination.

A calculation model for the operating cost of the pollutant removal system was established [22]–[24] based on the main equipment and structural components of the four pollutant removal systems of SCR, ESP, WFGD and WESP in the ULE system, analysis of the energy consumption and material consumption in the operation of each individual system.

A. OPERATION COST MODEL OF DENITRIFICATION

In a denitrification system, the main components of cost are energy and material consumption. The main factors in energy consumption include the power consumptions of the draft fan, the ash blower and the dilution fan. The relevant formulas are as follows:

$$COST_{idf\_SCR} = \frac{1}{q} \times \sqrt{3} cos\varphi \left(\sum_{i=1}^{n_{idf}} I_i U_i\right) \times P_E \times \alpha_{SCR} \quad (2\text{-}8)$$

$$COST_{sb} = \begin{cases} \dfrac{P_{steam}}{CV_s} \times CV + \sum_{i=1}^{n_{sb}} P_i \\ \dfrac{1}{6} \times \sum_{i=1}^{n_{sb}} P_i \end{cases} \quad (2\text{-}9)$$

$$COST_{adf} = \frac{1}{q} \times \sqrt{3} cos\varphi \left(\sum_{i=1}^{n_{adf}} I_i U_i\right) \times P_E \quad (2\text{-}10)$$

n_{idf}, n_{sb}, n_{adf} represent the operating numbers of the draft fan, blower and dilution fan, respectively.

U_i, I_i represent the voltage and current, respectively of the i-th device.

$cos\varphi$ represents the power factor, which in this study is assumed to be 0.8.

P_E represents the electricity price, which in this study is assumed to be 0.45 yuan/kWh.

q represents the real-time load of the boiler.

P_{steam} represents the energy consumption of empirical steam.

CV_s represents the empirical reference catalyst dosage.

CV represents the actual amount of catalyst.

α_{SCR} represents the ratio of the resistance of the denitrification reactor to the first half of the total resistance, the calculation method is as follow:

$$\alpha_{SCR} = \frac{p_{SCR}}{p_{idf}} \quad (2\text{-}11)$$

The main physical consumption of the denitrification system is the cost of liquid ammonia and catalyst. According to the material balance, the formula for liquid ammonia cost is:

$$COST_{NH_3} = \frac{1}{q} \times \left(c_{NOx_{in}} - c_{NO_{xout}}\right) \times V \times \frac{M_{NH3}}{M_{NO}} \times \frac{2}{3} \times \frac{1}{\delta_2} \times \frac{ae \times M_{NH3}}{V_m} \times P_{NH_3} \quad (2\text{-}12)$$

δ_2 represents the ammonia-to-nitrogen ratio.

P_{NH3} is the price of liquid nitrogen. This study assumes 3000 yuan/ton.

V represents the smoke flow.

The flue gas flow is positively correlated with the boiler load, which can be calculated with the following formula:

$$\mathrm{V} = m \times q \times V_{tc} \quad (2\text{-}13)$$

m is the power consumption of raw coal.

V_{tc} represents the amount of smoke burned by a unit of coal.

The formula for catalyst loss cost is as follow:

$$COST_C = \frac{CV \times P_c}{3Qh} \tag{2-14}$$

P_c represents the price of the catalyst. And This study assumes 30,000 yuan/ton.

Q represents the capacity of the unit. This study assumes 1000 MW. h is the number of annual operating hours of the unit. In accordance with the utilization time of China's thermal power in 2016, this study assumes 4000 hours [25].

The overall operating cost of the selective catalytic reduction denitrification system can be expressed as:

$$COST_{SCR} = COST_{idf\_SCR} + COST_{sb} + COST_{adf} + COST_{NH_3} + COST_C \tag{2-15}$$

B. OPERATION COST MODEL FOR DESULFURIZATION

In desulfurization systems, the main operation costs are energy consumption and material consumption. The main consumer of energy is the desulfurization system electrical equipment, including the booster fan, the oxidized fan, the oxidation slurry circulating pump, the slurry mixer, etc. Their cost formulas, respectively, are as follows:

$$COST_{bf} = \frac{1}{q} \times \sqrt{3} cos\varphi \left(\sum_{i=1}^{n_{bf}} I_i U_i \right) \times P_E \times \alpha_{WFGD} \tag{2-16}$$

$$COST_{sa} = \frac{1}{q} \times \sqrt{3} cos\varphi \left(\sum_{i=1}^{n_{sa}} I_i U_i \right) \times P_E \tag{2-17}$$

$$COST_{scp} = \frac{1}{q} \times \sqrt{3} cos\varphi \left(\sum_{i=1}^{n_{scp}} I_i U_i \right) \times P_E \tag{2-18}$$

$$COST_{oab} = \frac{1}{q} \times \sqrt{3} cos\varphi \left(\sum_{i=1}^{n_{oab}} I_i U_i \right) \times P_E \tag{2-19}$$

$n_{bf}, n_{sa}, n_{scp}, n_{oab}$ represent the number of operating platforms of the booster fan, the oxidation fan, the slurry circulating pump and the slurry agitator, respectively.

$p_{WESP}, p_{dt}, p_{gd2}$ represent the pressure drop of the desulfurization tower, the resistance pressure drops of the wet electrostatic precipitator and the partial resistance pressure drop of the flue, respectively.

α_{WFGD} represents the ratio of the desulfurization tower resistance to the latter half of the total resistance. The calculation method is defined as follows:

$$\alpha_{WFGD} = \frac{p_{dt}}{p_{dt} + p_{WESP} + p_{gd2}} \tag{2-20}$$

In the formula, the desulfurization absorber of the limestone-gypsum wet desulfurization system is limestone slurry. According to the material balance, the unit power generation cost is:

$$COST_{CaCO_3} = \frac{1}{q} \times \left(c_{SO_2\_in} - c_{SO_2\_out} \right) \times V \times \frac{M_{CaCO_3}}{M_{SO_2}} \times \frac{\delta_1}{\lambda} \times P_{CaCO_3} \tag{2-21}$$

δ_1 represents the calcium to sulfur ratio;

λ represents the purity of limestone. This study assumes 90%.

P_{CaCO_3} represents limestone price. This study assumes 500 yuan/ton.

In addition to limestone consumption, material consumption also includes the consumption cost of process water. The formula is:

$$COST_w = \frac{1}{q} \times \left(c_{SO_2\_in} - c_{SO_2\_out} \right) \times V \times \frac{M_{CaCO_3}}{M_{SO_2}} \times \frac{\delta_1}{\lambda} \times \frac{2M_{H_2O}}{M_{CaCO_3}} \times P_w \tag{2-22}$$

The limestone-gypsum wet desulfurization system produces the byproduct gypsum while removing the flue gas. Gypsum is included in the cost calculation as a benefit in the operation of the desulfurization system, and its earnings formula is as follow:

$$R_{CaSO_4} = \frac{1}{q} \times \left(c_{SO_2\_in} - c_{SO_2\_out} \right) \times V \times \frac{M_{CaSO_4}}{M_{SO_2}} \times P_{CaSO_4} \tag{2-23}$$

P_{CaSO_4} represents the price of gypsum. This study assumes 500 yuan/ton.

The total operation cost of wet limestone-gypsum desulfurization can be expressed as:

$$COST_{WFGD} = COST_{bf} + COST_{sa} + COST_{scp} + COST_{oab} + COST_{CaCO_3} + COST_w - R_{CaSO_4} \tag{2-24}$$

C. OPERATION COST MODEL FOR DEDUSTING

The main operation cost of the electric precipitator is electricity consumption. The electricity consumption of the dry electrostatic precipitator is primarily the power consumption of the draft fan and the power consumption of the power supply. The formulas for these costs are as follows:

$$COST_{idf\_ESP} = \frac{1}{q} \times \sqrt{3}\, cos\varphi \left(\sum_{i=1}^{n_{idf}} I_i U_i \right) \times P_E \times \alpha_{ESP} \tag{2-25}$$

$$COST_e = \frac{1}{q} \times \sqrt{3} cos\varphi \left(\sum_{i=1}^{n_e} I_i U_i \right) \times P_E \tag{2-26}$$

n_e represents the number of electric fields.

α_{ESP} represents the ratio of electrostatic precipitator resistance to the first half of the total resistance. The formula for calculating it is:

$$\alpha_{ESP} = \frac{p_{ESP}}{p_{idf}} \tag{2-27}$$

The operating cost of an electrostatic precipitator is:

$$COST_{ESP} = COST_{idf\_ESP} + COST_e \tag{2-28}$$

The electricity consumption of the induced draft fan of the wet electrostatic precipitator is related to the ratio of its resistance to the first half of the resistance. The method for calculating the cost is as follow:

$$COST_{idf\_WESP} = \frac{1}{q} \times \sqrt{3}\, cos\varphi \left(\sum_{i=1}^{n_{idf}} I_i U_i \right) \times P_E \times \alpha_{WESP} \tag{2-29}$$

$$\alpha_{WESP} = \frac{p_{WESP}}{p_{idf}} \tag{2-30}$$

Compared with the dry electrostatic precipitator, the wet electrostatic precipitator has greater power consumption cost and material cost, and the increased power consumption cost is mainly due to the power consumption of the water circulation system. Its formula is as follows:

$$COST_{wc} = \frac{1}{q} \times \sqrt{3} cos\varphi \left(\sum_{i=1}^{n_{wc}} I_i U_i \right) \times P_E \quad (2\text{-}31)$$

The main components of the material cost of the wet electrostatic precipitator are the process water cost and the alkali consumption cost. The method of calculating these is as follows:

$$COST_w = \frac{1}{q} \times w \times P_w \quad (2\text{-}32)$$

$$COST_{Na} = \frac{1}{q} \times Na \times P_{Na} \quad (2\text{-}33)$$

The operation cost of the wet electric dust removal system can be expressed as:

$$COST_{WESP} = COST_{idf\_WESP} + COST_e + COST_w + COST_{Na} + COST_{wc} \quad (2\text{-}34)$$

III. COLLABORATIVE OPTIMIZATION METHOD FOR A ULE SYSTEM WITH A DYNAMIC PENALTY FUNCTION

A. IMPROVED COLLABORATIVE OPTIMIZATION WITH A DYNAMIC PENALTY FUNCTION

The collaborative optimization algorithm decomposes a complex model into a system level and a discipline level. Compared with the original complex model, the discipline level contains several relatively simple sub models, which include only partial variables and constraints. The optimization of each discipline does not consider variables and constraints that are not related to the discipline, which reduces the difficulty of solution. The objective of the system level is to coordinate the coupled variables between disciplines and obtain the global optimal solution under the constraints of consistency of coupled variables.

1) THE SYSTEM LEVEL IMPROVEMENT OF COLLABORATIVE OPTIMIZATION

The system level optimization of standard CO can be expressed as follows:

$$\begin{aligned} &\text{Min } f = f(z) \\ &\text{s.t. } J_i(z) = \sum_{j=1}^{n_i} (x_{ij}^* - z_{ij})^2 = 0, \quad i = 1...N \end{aligned} \quad (3\text{-}1)$$

f represents the target function of the system.

z represents a system level design variable, and z_{ij} represents the j-th system level design variable, that is assigned to the i-th discipline.

x^* represents an optimal solution for the discipline level optimization design variable, of which there are a total of N. x_{ij}^* represents the optimal solution of the j-th design variable, which is returned from the i-th disciplinary level optimization.

J represents a system level nonlinear constraint, of which there are a total of N.

n_i represents the number of design variables assigned at the system level to the i-th discipline level optimization.

The purpose of the system level is to optimize the objective function of the problem and to coordinate the inconsistencies among disciplines. Only when the optimal solution at each discipline level is the same as the expected solution at the system level is consistency between the disciplines reached. However, the difficulty of calculating CO is mainly due to the system level optimization. Therefore, the expression of the system level has been adjusted by a dynamic penalty function in this paper. To ensure that the system level optimization is feasible and has a solution, each constraint can be taken as a penalty term and added to the system level objective function. The disciplinary inconsistency is reflected by the penalty term in the objective function. In addition, the penalty function forces the optimization results toward reduced disciplinary inconsistency at the system level, so that the expected value passed to the discipline level can better meet the constraints of each discipline. In this way, it is easier to find a global optimal solution that satisfies the consistency requirements between disciplines after multiple iterations. The system level optimization formula is shown in equation (3-2).

$$\text{Min } F(z) = f(z) + \gamma \sum_{i=1}^{n} J_i(z) \quad (3\text{-}2)$$

$f(z)$ represents the original system level objective function.

γ represents the penalty factor.

$J_i(z)$ represents the interdisciplinary consistency constraint.

The performance of the penalty function method in dealing with the constraint problem depends largely on the choice of penalty factor γ. Therefore, a fixed penalty factor is not suitable for solving this problem, and a dynamically adjustable penalty factor should be adopted.

When the penalty factor is too large, the rate of decline of the objective function value decreases. When the penalty factor is too small, the inconsistency between disciplines increases. Therefore, the dynamically adjusted penalty factor has better adaptability than the fixed value. In collaborative optimization, it is expected that with the iterative process, the amount of inconsistent information between disciplines is gradually reduced, and the objective function value gradually converges to the optimal value. Therefore, the expression of the dynamic penalty function can be constructed by using inconsistent information between disciplines. When there is a large amount of disciplinary inconsistency, the discipline consistency constraint is given a greater weight to maintain consistency between disciplines. When there is a small amount of disciplinary inconsistency, the interdisciplinary consistency constraint is given a smaller weight to converge to a minimum value faster. The dynamic penalty factor expression constructed is shown in equation (3-3).

$$\gamma = b + m * k^{\alpha} \quad (3\text{-}3)$$

where b, m and α are constant. When the inconsistency between disciplines is very small, the b value is used to maintain discipline consistency in the objective function. When the system level assigned design vector expectation is within the feasible domain, the system level optimization is carried out in the feasible region via the b value, which can effectively enhance the robustness of the algorithm. The role of m and α is to control the weight of the consistency constraint among disciplines, which can be selected according to the system level objective function of the optimization problem and the magnitude of the design variables. k represents the inconsistent information among subjects.

2) THE IMPROVEMENT OF DISCIPLINE LEVEL COLLABORATIVE OPTIMIZATION

The discipline level of collaborative optimization can be expressed as follows:

$$\begin{aligned} &\text{Min } J_i(x) = \sum_{j=1}^{n_i} (x_{ij} - z_{ij})^2 \\ &\text{s.t. } h_{id}(x) < 0 \\ &\quad g_{ie}(x) = 0 \end{aligned} \tag{3-4}$$

x represents the optimization design variable at the discipline level.

h_{id} is the inequality constraint for optimization of discipline i, of which there are a total of d.

g_{ie} represents the equality constraints for optimization of discipline i, of which there are a total of e.

The objective function of discipline level optimization is the sum of least squares, and it is expected that the discipline level variables are close to the objective variables allocated by the system level. Because an objective function at the discipline level does not consider the optimal design points of the other disciplines, it is easy to fall into a local optimal solution. Therefore, in this paper, the part of the system's objective function corresponding to a discipline is added to the discipline level to widen the optimization space and reduce dependence on the initial point. The optimization formula for a discipline level is given by equation (3-5).

$$\begin{aligned} &\text{Min } J_i(x) = \sum_{j=1}^{n_i} (x_{ij} - z_{ij})^2 + \beta * f_i'(x) \\ &\text{s.t. } h_{id}(x) < 0, \quad g_{ie}(x) = 0 \end{aligned} \tag{3-5}$$

$f_i'(x)$ represents the discipline's part of the system's objective function.

β represents the weight factor, whose value is:

$$\beta = (z^t - z^{t-1})^2 \tag{3-6}$$

z^t represents the current system level design variable, and z^{t-1} represents the previous system level design variable.

B. COST OPTIMIZATION OF ULE SYSTEM BASED ON IMPROVED COLLABORATIVE OPTIMIZATION

The ULE system is optimized within the framework of collaborative optimization, which is shown in Fig. 2.

In the improved collaborative optimization framework, the ULE system is composed of a system level and three discipline levels (denitration, desulfurization and dedusting). In addition, the discipline objective is to minimize the difference between system level design variables under the constraints of their respective domains. The system level objective is to minimize operation cost while maintaining consistency between coupled variables.

1) SYSTEM LEVEL

The system level minimizes the sum of the operation costs of denitration, desulfurization and dedusting, which is expressed by equation (3-7).

$$\begin{aligned} &\text{Min } F(z) = COST_{SCR} + COST_{WFGD} + COST_{ESP} \\ &\qquad + COST_{WESP} + \gamma \sum_{i=1}^{3} J_i(z) \\ &\text{s.t. } 50 < z_1 < 150 \\ &\quad 40 \le z_2, z_3, z_4, z_5 \le 80 \\ &\quad 5.0 \le z_6 \le 5.6; z_7 = 2, 3, 4; \\ &\quad 30 \le z_8 \le 40 \end{aligned} \tag{3-7}$$

$z_1 - z_8$ represent the system level design variables. z_1 represents the amount of ammonia sprayed in the SCR. $z_2 - z_5$ represent the voltage of four electric fields in the ESP. z_6 and z_7, respectively, represent the pH value of gypsum slurry and the number of circulating pumps in the WFGD. z_8 represents the electric field voltage in the WESP. The constraints on the range of each variable in $z_1 - z_8$ are derived from its process constraints. The penalty term $\gamma \sum_{i=1}^{3} J_i(z)$ is derived from three equality constraints (3-8), (3-9) and (3-10).

$$\begin{aligned} J_1(z) &= (x_{11}^* - z_1)^2 + (x_{16}^* - z_6)^2 \\ &\quad + (x_{17}^* - z_7)^2 \end{aligned} \tag{3-8}$$

$$\begin{aligned} J_2(z) &= (x_{26}^* - z_6)^2 + (x_{27}^* - z_7)^2 \\ &\quad + (x_{28}^* - z_8)^2 \end{aligned}$$

$$\begin{aligned} J_3(z) &= (x_{32}^* - z_2)^2 + (x_{33}^* - z_3)^2 + (x_{34}^* - z_4)^2 + (x_{35}^* - z_5)^2 \\ &\quad + (x_{36}^* - z_6)^2 + (x_{37}^* - z_7)^2 + (x_{38}^* - z_8)^2 \end{aligned} \tag{3-9}$$

(3-10)

$x_{ij}^* (i = 1, 2, 3; j = 1, 2, \ldots, 8)$ is the optimization value returned to the system level from the discipline level.

2) DENITRATION DISCIPLINE

The objective function of the denitration discipline is to minimize the difference between its disciplinary design variables and the expected value from the system level. Furthermore, the part of the system objective function corresponding to the denitration discipline is added to the objective function. The objective function of the denitration discipline is expressed as

$$\begin{aligned} &\text{Min } J_1(x_1) = (x_{11} - z_1^*)^2 + (x_{16} - z_6^*)^2 + (x_{17} - z_7^*)^2 \\ &\qquad + \beta^* COST_{NOx\_removal} \\ &\text{s.t. } C_{NOx\_out} \le 50 \\ &\quad 50 \le x_{11} \le 150; 5.0 \le x_{16} \le 5.6; \\ &\quad x_{17} = 2, 3, 4 \end{aligned} \tag{3-11}$$

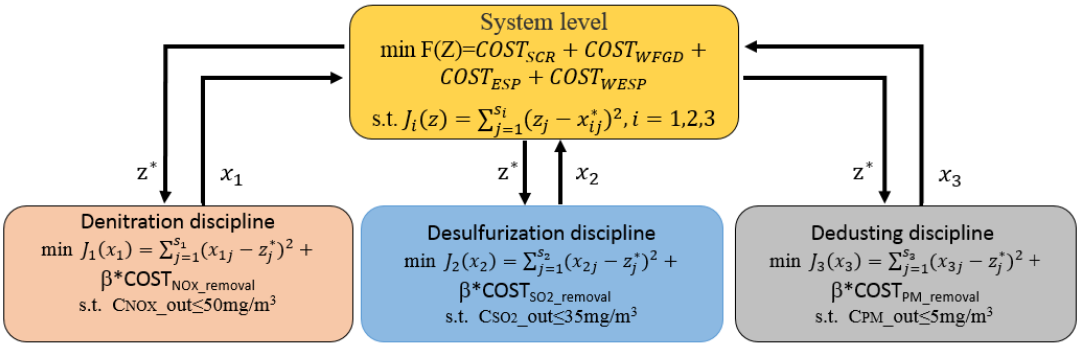

FIGURE 2. Improved collaborative optimization framework for the ULE system.

x_{11}, x_{16}, x_{17} are the design variables of the denitration discipline, and $z_1^* z_6^*$, z_7^* are the expected values of the design variables assigned to the denitrification discipline at the system level.

3) DESULFURIZATION DISCIPLINE

The objective function of the desulfurization discipline is to minimize the difference between its disciplinary design variables and the expected value from the system level. Furthermore, the part of the system objective function corresponding to the desulfurization discipline is added. The objective function of the desulfurization discipline is expressed as

$$\begin{aligned} \text{Min } J_2(x_2) &= (x_{26} - z_6^*)^2 + (x_{27} - z_7^*)^2 + (x_{28} - z_8^*)^2 \\ &\quad + \beta^* COST_{SO_2\_removal} \\ \text{s.t. } & C_{SO_2\_out} \leq 35 \\ & 5.0 \leq x_{26} \leq 5.6;\ x_{27} = 2, 3, 4 \\ & 30 \leq x_{28} \leq 40 \end{aligned} \tag{3-12}$$

x_{26}, x_{27}, x_{28} are the design variables of the desulfurization discipline, and z_6^*, z_7^*, z_8^* are the expected values of the design variables assigned to the desulfurization discipline at the system level.

4) DEDUSTING DISCIPLINE

The objective function of the dedusting discipline is to minimize the difference between its disciplinary design variables and the expected value from the system level. Furthermore, the part of the system objective function corresponding to the dedusting discipline is added. The objective function of the dedusting discipline is expressed as

$$\begin{aligned} \text{Min } J_3(x_3) &= (x_{32} - z_2^*)^2 + (x_{33} - z_3^*)^2 + (x_{34} - z_4^*)^2 \\ &\quad + (x_{35} - z_5^*)^2 + (x_{38} - z_8^*)^2 \\ &\quad + \beta^* COST_{PM\_removal} \\ \text{s.t. } & C_{PM\_out} \leq 5 \\ & 40 \leq x_{32}, x_{33}, x_{34}, x_{35} \leq 80; \\ & 5.0 \leq x_{36} \leq 5.6;\ x_{37} = 2, 3, 4;\ 30 \leq x_{38} \leq 40 \end{aligned} \tag{3-13}$$

$x_{32}, x_{33}, x_{34}, x_{35}, x_{38}$ are the design variables of the dedusting discipline, and $z_2^*, z_3^*, z_4^*, z_5^*, z_8^*$ are the expected values of the design variables assigned to the dedusting discipline at the system level.

The flow chart of the improved collaborative optimization of the ULE system is shown in Fig.3.

The process of improved collaborative optimization of the ULE system is as follows:

Step 1 The parameters for collaborative optimization are set and the system level design variables are initialized.

Step 2 The system level variables are assigned to each discipline, and the initial values of the discipline design variables are combined so they can be solved by the respective discipline level optimizer.

Step 3 The optimal solution for each discipline level is transmitted back to the system level.

Step 4 If the conditions are met, the optimization is terminated. Otherwise, the optimal solution of the design variable at the current system level is assigned to each discipline for a new round of optimization.

Step 5 Repeat Step 2 to Step 4 until the condition for suspension of optimization is satisfied.

In the optimization process, the convergence condition of the collaborative optimization algorithm is $\left|z^k - z^{k-1}\right| \leq \theta$. This means that the system level has little space for optimization, and the current result can be regarded as the global optimal solution.

IV. CASE STUDIES

In this study, the boiler for a 1000 MW unit was taken as the research object, and the simulation was carried out with loads of 50%, 75% and 100%. First, improved collaborative optimization (ICO) is compared with relaxation based collaborative optimization (RCO) [26]. In addition, the simulation data of the ULE system based on ICO are presented. Finally, a simulation of the ULE system was used to compare ICO and PSO (particle swarm optimization). In this paper, different working conditions are taken as research cases, as shown in Table 1.

To verify the effectiveness of the algorithm, ICO and RCO are compared in different cases. The comparison results are shown in Table 2. It can be concluded that ICO can find a lower operating cost than RCO under various conditions.

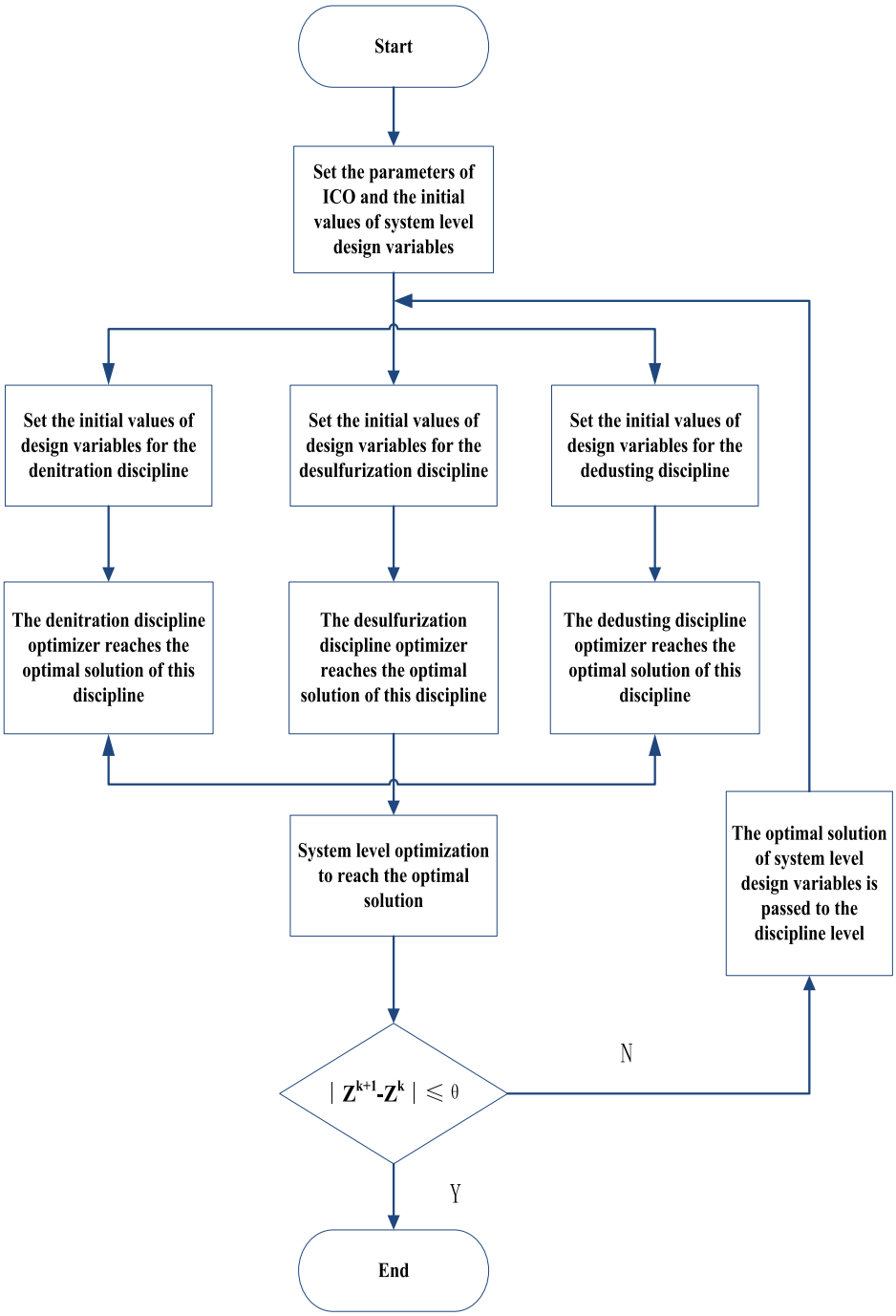

FIGURE 3. Flow chart for improved collaborative optimization the ULE system.

Taking condition 5 as an example, three initial points of z1 = [5 40 20 20 40 5 2 30], z2 = [65 80 80 80 5 4 45] and z3 = [40 50 50 50 50 5 2 40] are simulated with RCO and ICO. The iterative processes are shown in Fig. 4. The graph shows that the number of ICO iterations is larger, but the algorithm is less affected by the initial point and has better global optimization performance. Therefore, ICO can find better operating costs than RCO.

Fig. 5 shows the iterative process of ICO at the system level and discipline level. In the figure, operation cost is optimized at the system level and the objective function of the discipline level gradually approaches zero through iteration. This shows that the inconsistency between disciplines decreases as the coordination of the system level increases, until the optimal solution is found.

Fig. 6 shows the removal process of all pollutants in the ULE system under condition 9. The concentration of

TABLE 1. Comparison table of operating conditions.

Working condition	Description of working conditions	Load （MW）	Concentration of inlet SO_2 （mg/m^3）	Concentration of inlet NO_x （mg/m^3）	Concentration of inlet PM （mg/m^3）
condition 1	Low load, low pollutant concentration	500	600	100	800
condition 2	Low load, medium pollutant concentration	500	1000	200	1200
condition 3	Low load, high pollutant concentration	500	1200	250	1600
condition 4	Medium load, low pollutant concentration	750	600	100	800
condition 5	Medium load, medium pollutant concentration	750	1000	200	1200
condition 6	Medium load, high pollutant concentration	750	1200	250	1600
condition 7	High load, low pollutant concentration	1000	600	100	800
condition 8	High load, medium pollutant concentration	1000	1000	200	1200
condition 9	High load, high pollutant concentration	1000	1200	250	1600

TABLE 2. Comparison results between RCO and ICO.

Working condition	Optimization algorithm	Concentration of outlet NO_x （mg/m^3）	Concentration of outlet SO_2 （mg/m^3）	Concentration of outlet PM （mg/m^3）	Operation cost （yuan/kWh）
Condition 1	RCO	50.00	1.36	4.99	0.027428
	ICO	50.00	2.02	5.00	0.027283
Condition 2	RCO	49.99	2.27	5.00	0.028177
	ICO	50.00	3.78	5.00	0.028032
Condition 3	RCO	49.97	2.73	5.00	0.028531
	ICO	50.00	4.90	5.00	0.028383
Condition 4	RCO	49.99	2.59	4.99	0.024363
	ICO	50.00	3.90	5.00	0.024257
Condition 5	RCO	49.80	6.81	5.00	0.025183
	ICO	50.00	10.06	5.00	0.025002
Condition 6	RCO	49.99	4.31	5.00	0.02548
	ICO	50.00	13.72	5.00	0.02535
Condition 7	RCO	50.00	3.90	5.00	0.022827
	ICO	50.00	6.11	5.00	0.022742
Condition 8	RCO	49.99	6.51	5.00	0.023572
	ICO	50.00	15.94	5.00	0.023483
Condition 9	RCO	50.00	7.88	4.99	0.023922
	ICO	50.00	18.31	5.00	0.023832

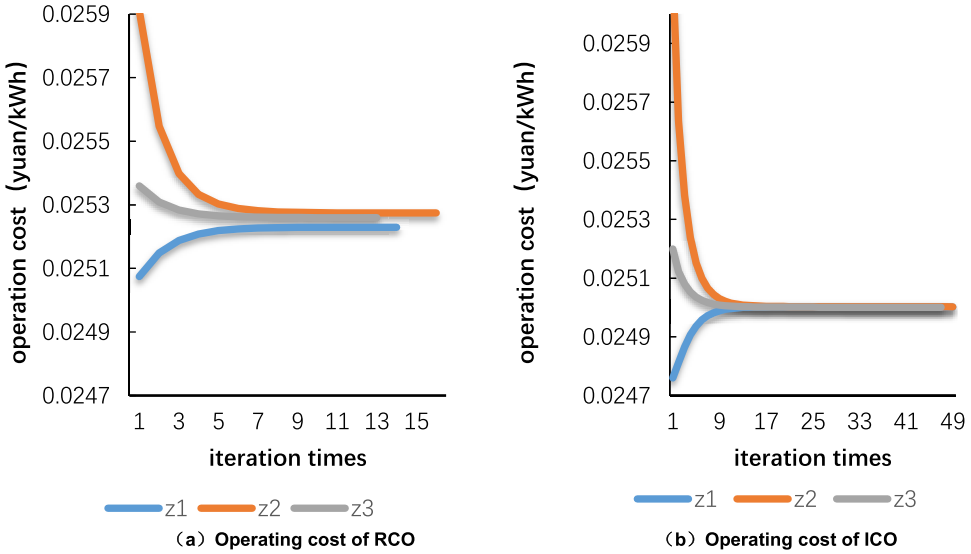

FIGURE 4. Comparison of operating costs between RCO and ICO.

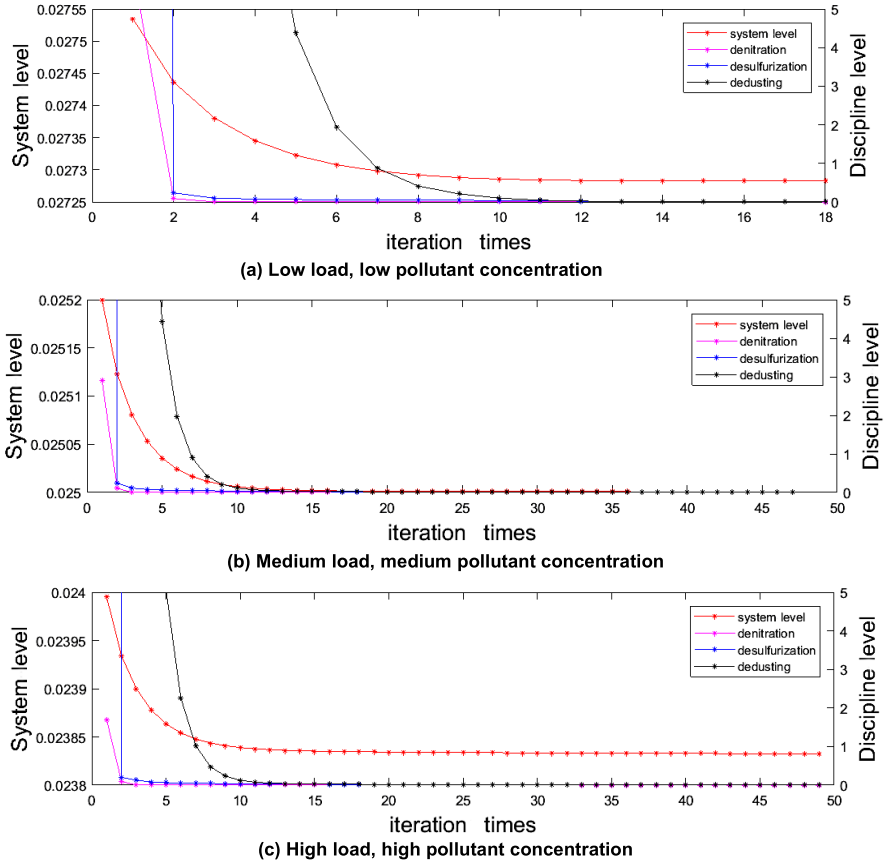

FIGURE 5. Iterative process of ICO.

NOx decreased to 55.7 mg/m^3 after passing SCR and was decreased to 50 mg/m^3 via the synergistic removal of WFGD. The PM removal efficiency of ESP is more than 99%, and the PM concentration at the exit is only 43.7 mg/m^3. Finally, the PM concentration in the flue gas was reduced to 5.0 mg/m^3 by WFGD and WESP. SO_2 was mainly removed by WFGD. When the flue gas passed through the WFGD system, the concentration of SO_2 was 26.2 mg/m^3. Subsequently, the concentration of SO_2 was reduced to 18.3 mg/m^3 via the synergistic removal of WESP.

Fig. 7 compares the overall operation costs of the ULE system based on ICO under different conditions. The results

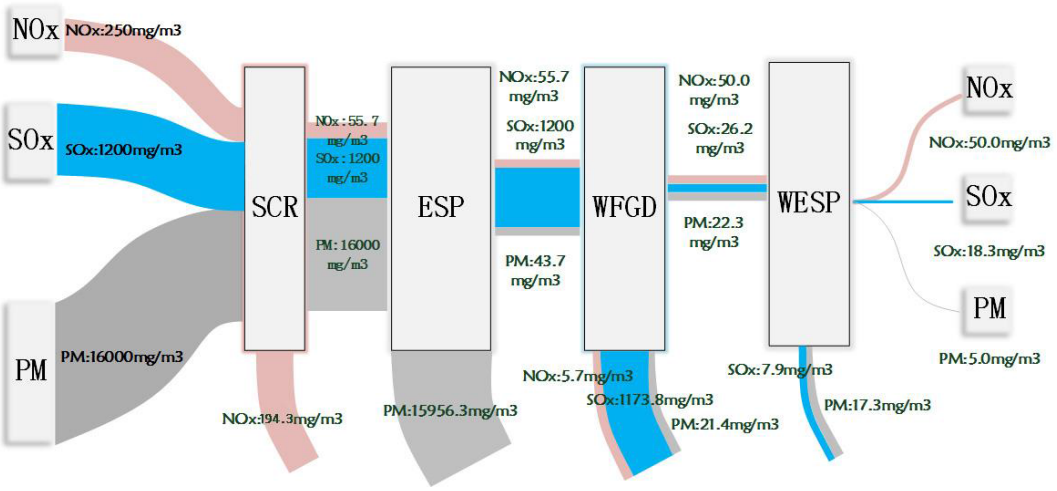

FIGURE 6. The pollutant removal process of the ULE system under condition 9.

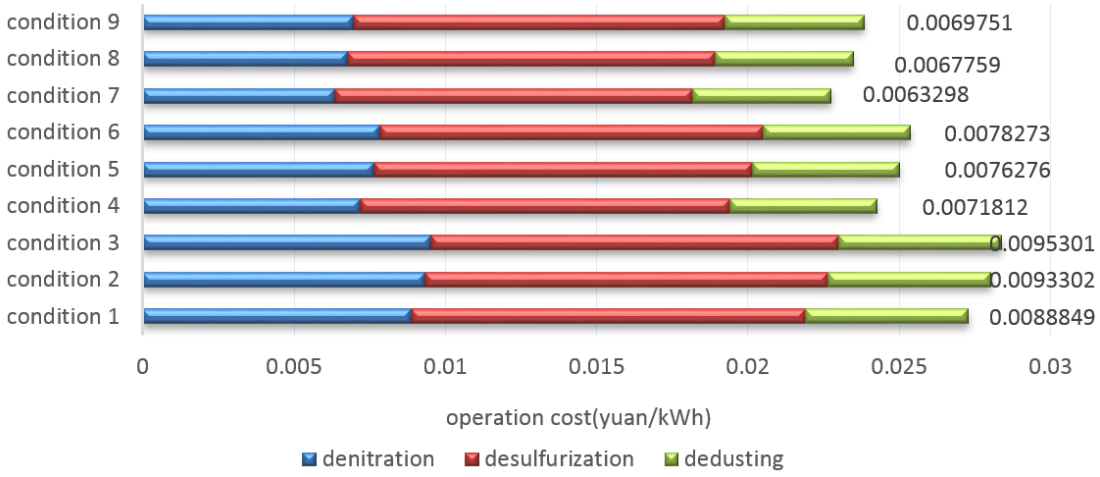

FIGURE 7. Comparison of operation costs under different conditions.

show that the operation cost of condition 3 with low load and high pollutant concentration is the highest, at 0.028383 yuan/kWh. The operation cost of condition 7 with high load and low pollutant concentration is the lowest, at 0.022742 yuan/kWh. In general, the operation cost decreases with increasing load and increases with increasing pollutant concentration.

To prove the advantages of collaborative removal and decentralized decision in the ULE system, the following three strategies are compared. The first strategy is to obtain the optimal operation cost by independent optimization (IO) without consideration of collaborative removal among devices. The second strategy considers the collaborative removal among devices and uses centralized decision, which is solved by particle swarm optimization (PSO). The third strategy considers the collaborative removal among devices and uses decentralized decision solved by ICO. The results of comparing these strategies are shown in Table 3. In addition, the annual (8000 hours) cost estimates for the three strategies under different conditions are shown in Table 4.

Table 4 shows that the operation cost obtained by independent optimization is significantly higher than the other strategies under all conditions. Furthermore, the optimal solution found by ICO for each condition found by ICO is the lowest, with an average cost savings of 500,000 yuan. Although there is not much difference between centralized decision by PSO and decentralized decision by ICO, centralized decision is difficult to solve, and the possibility of finding a solution by PSO becomes less certain as the problem complexity increases. Repeatability simulations are carried out for centralized decision via PSO under condition 2 and are shown in Table 5.

It can be seen from Table 5 that PSO has a large fluctuation, and the optimal results form PSO-2 are even worse than the results by independent optimization in Table 3. Therefore, compared with centralized decision, it is easier to find the optimal solution of the system by ICO.

TABLE 3. Comparison results of the three strategies for the ULE system.

Working condition	IO (yuan/kWh)	centralized decision by PSO (yuan/kWh)	decentralized decision by ICO (yuan/kWh)
Condition 1	0.027398	0.027289	0.027283
Condition 2	0.028140	0.028035	0.028032
Condition 3	0.028486	0.028386	0.028383
Condition 4	0.024340	0.024289	0.024257
Condition 5	0.025069	0.025007	0.025002
Condition 6	0.02543	0.025362	0.02535
Condition 7	0.022807	0.022746	0.022742
Condition 8	0.023552	0.023485	0.023483
Condition 9	0.02389	0.023845	0.023832

TABLE 4. Comparison of annual operation cost of units (ten thousand yuan).

Working condition	IO	PSO	ICO
Condition1	10959.2	10915.6	10913.2
Condition2	11256.0	11214.0	11212.8
Condition3	11394.4	11354.4	11353.2
Condition4	14604.0	14573.4	14554.2
Condition5	15041.4	15004.2	15001.2
Condition6	15258.0	15217.2	15210.0
Condition7	18245.6	18196.8	18193.6
Condition8	18841.6	18788.0	18786.4
Condition9	19112.0	19076.0	19065.6

TABLE 5. Repeatability simulations for centralized decision via PSO in condition 2.

Operation parameter	PSO	PSO-1	PSO-2	PSO-3
Spray amount of ammonia (kg/h)	55.38	57.24	56.84	57.30
#1 field secondary voltage (kV)	45.98	41.01	40.00	42.99
#2 field secondary voltage (kV)	35.39	37.74	40.18	44.38
#3 field secondary voltage (kV)	41.94	42.56	30.89	34.97
#4 field secondary voltage (kV)	40.00	40.00	49.43	40.00
Slurry pH	5.0	5.6	5.6	5.6
Number of circulating pump stations	2	2	2	2
Wet secondary voltage (kV)	30.00	30.00	35.47	31.28
Operation cost (yuan/kWh)	0.028035	0.028041	0.028184	0.028044
Concentration of outlet NO_x (mg/m^3)	49.94	49.80	49.70	49.86
Concentration of outletSO_2 (mg/m^3)	6.87	2.27	2.69	2.27
Concentration of outlet PM (mg/m^3)	5.00	4.99	3.42	4.85

V. CONCLUSION

This article proposes a method for optimizing operation cost for ultralow emission systems in coal-fired power plants based on improved CO. First, a model for the operation cost of a ULE system is introduced. Second, the function for improved collaborative optimization with dynamic penalty

and the model of the ULE system based on ICO are presented. Finally, the simulation results show that the proposed operation cost optimization method for a ULE system is competitive in global optimization and in terms of practicality. In future work, we will extend the proposed idea to solve other complex problems in science and engineering.

REFERENCES

[1] H. Peng, W. Gui, H. Shioya, and R. Zou, "A predictive control strategy for nonlinear NOx decomposition process in thermal power plants," *IEEE Trans. Syst., Man, Cybern. A, Syst., Humans*, vol. 36, no. 5, pp. 904–921, Sep. 2006.
[2] H. Peng, K. Nakano, and H. Shioya, "Nonlinear predictive control using neural nets-based local linearization ARX model—Stability and industrial application," *IEEE Trans. Control Syst. Technol.*, vol. 15, no. 1, pp. 130–143, Jan. 2007.
[3] A. L. V. Perales, P. Ollero, F. J. G. Ortiz, and A. Gómez-Barea, "Model predictive control of a wet limestone flue gas desulfurization pilot plant," *Ind. Eng. Chem. Res.*, vol. 48, no. 11, pp. 5399–5405, Jun. 2009.
[4] W. F. Li, "The flue gas desulfurization control based on control algorithm of improved neural network PID," M.S. thesis, Taiyuan Univ. Technol., Taiyuan, China, 2009.
[5] G. F. Xu, "Energy-saving optimization and controller design for industrial electrostatic precipitator equipment," M.S. thesis, Dalian Univ. Technol., Dalian, China, 2009.
[6] N. Grass, "Fuzzy-logic-based power control system for multifield electrostatic precipitators," *IEEE Trans. Ind. Appl.*, vol. 38, no. 5, pp. 1190–1195, Sep. 2002.
[7] Z. Li, C. Shao, Y. An, and G. Xu, "Energy-saving optimal control for a factual electrostatic precipitator with multiple electric-field stages based on GA," *J. Process Control*, vol. 23, no. 8, pp. 1041–1051, Sep. 2013.
[8] J. Yeoman and M. Duckham, "Decentralized detection and monitoring of convoy patterns," *Int. J. Geograph. Inf. Sci.*, vol. 30, no. 5, pp. 993–1011, Nov. 2015.
[9] C. Horch, M. Gulde, N. Scherer-Negenborn, K. Stein, C. Schweitzer, and N. Wendelstein, "Nanosat-based detection and tracking of launch vehicles," *Proc. SPIE*, vol. 10794, Oct. 2018, Art. no. 107940L.
[10] C. R. F. de Almeida, L. Weigang, G. V. Meinerz, and L. Li, "Satisficing game approach to collaborative decision making including airport management," *IEEE Trans. Intell. Transp. Syst.*, vol. 17, no. 8, pp. 2262–2271, Aug. 2016.
[11] J. Alonso-Mora, S. Baker, and D. Rus, "Multi-robot formation control and object transport in dynamic environments via constrained optimization," *Int. J. Robot. Res.*, vol. 36, no. 9, pp. 1000–1021, Aug. 2017.
[12] Y. Yin, H. Niu, and X. Liu, "Adaptive neural network sliding mode control for quad tilt rotor aircraft," *Complexity*, vol. 2017, Oct. 2017, Art. no. 7104708.
[13] A. Belegundu, E. Halberg, M. Yukish, and T. Simpson, "Attribute-based multidisciplinary optimization of undersea vehicles," in *Proc. 8th Symp. Multidisciplinary Anal. Optim.*, Aug. 2012, p. 4865.
[14] Y. Guang-Qiu, L. Shu-Wen, and D. B. Perlurst, "Multidisciplinary design and collaborative optimization for excavator backhoe device," *J. Eng. Sci. Technol. Rev.*, vol. 7, no. 2, pp. 99–105, 2014.
[15] H. Li, M. Ma, and W. Zhang, "Improving collaborative optimization for MDO problems with multi-objective subsystems," *Struct. Multidisciplinary Optim.*, vol. 49, no. 4, pp. 609–620, Oct. 2013.
[16] Q. Yang and W. Deyu, "Optimization design of ship engine room structures based on sectionalized dynamic relaxation collaborative optimization method," *Chin. J. Ship Res.*, vol. 11, no. 6, pp. 40–46, 2016.
[17] S. Zheng, J. Gao, and J. Xu, "Research on production planning and scheduling based on improved collaborative optimization," *Concurrent Eng.*, vol. 27, no. 2, pp. 99–111, Apr. 2019.
[18] B.-S. Jang, Y.-S. Yang, H.-S. Jung, and Y.-S. Yeun, "Managing approximation models in collaborative optimization," *Struct. Multidisciplinary Optim.*, vol. 30, no. 1, pp. 11–26, Jan. 2005.
[19] Y. Zhong, "Theoretical and experimental study of simultaneous removal of sulfur, nitrogen and mercury pollutant in WFGD system," Ph.D. dissertation, Zhejiang Univ., Hangzhou, China, 2008.
[20] J. Zhang, "Mechanism and model study on high efficiency desulfurization and dedust based on ultra-low emission technology," Ph.D. dissertation, Zhejiang Univ., Hangzhou, China, 2018.
[21] Z. D. Yang, C. H. Zheng, and X. Gao, "Experimental study on simultaneous control of SO_2 and PM by Wet electrostatic precipitato," *J. Eng. Thermophys.*, vol. 36, no. 6, pp. 1365–1370.2015.
[22] J. Y. Shi, "Cost-benefit analysis of desulfurization and denitration technologies for coal-fired power plants," M.S. thesis, Zhejiang Univ., Hangzhou, China, 2015.
[23] K. Jin, "Study on cost-benefit of environmental protection equipment in coal-fired power plants," M.S. thesis, Zhejiang Univ., Hangzhou, China, 2016.
[24] Z. W. Xu, "Study on operating optimization of coal-fired unit ultralow emission system. Master thesis," Zhejiang Univ., Hangzhou, China, 2108.
[25] *Annual Development Report of China Electric Power Industry 2017*, China Electr. Council, Beijing, China, 2017.
[26] J. Chen, Y. C. Lu, and L. M. Wang, "Dynamic relaxation cooperative optimization method with fast convergence," *J. Syst. Simul.*, vol. 30, no. 1, pp. 96–104, 2018.

SONG ZHENG was born in Guizhou, China, in 1982. He received the B.S., M.S., and Ph.D. degrees in control science and engineering from Zhejiang University, China, in 2008.

He is currently an Associate Researcher with the Automation College, Hangzhou Dianzi University. His research interest includes industrial automation, modeling, and optimization.

KAFEI TANG was born in Fuyang, Anhui, China, in 1994. He received the B.S. degree in automation from the Tongling University of Engineering, Anhui, in 2017. He is currently pursuing the master's degree with the School of Automation, Hangzhou Dianzi University, Zhejiang, China. His research direction is industrial optimization.

SHUAI CHEN was born in Shaoxing, Zhejiang, China, in 1994. He received the B.S. degree in automation from Hangzhou Dianzi University, Zhejiang, China, in 2017, where he is currently pursuing the master's degree with the School of Automation. His research interest includes industrial automation and optimization.

XIAOQING ZHENG was born in Zhejiang, China, in 1981. She received the B.S. and M.S. degrees in control science and engineering from Zhejiang University, China, in 2006.

From April 2006 to October 2008, she was a Senior Research Engineer with Honeywell (China) Company, Ltd. Since November 2008, she has been an Assistant Researcher with the Automation College, Hangzhou Dianzi University. Her research interest includes industrial process modeling and optimization.